SUPPLEMENTARY INFORMATION

An efficient protocol for CUT&RUN analysis of FACS-isolated mouse satellite cells

Kamar Ghaibour#, Joe Rizk#, Claudine Ebel, Tao Ye, Muriel Philipps, Valérie Schreiber, Daniel Metzger, Delphine Duteil

SUPPLEMENTARY FIGURES

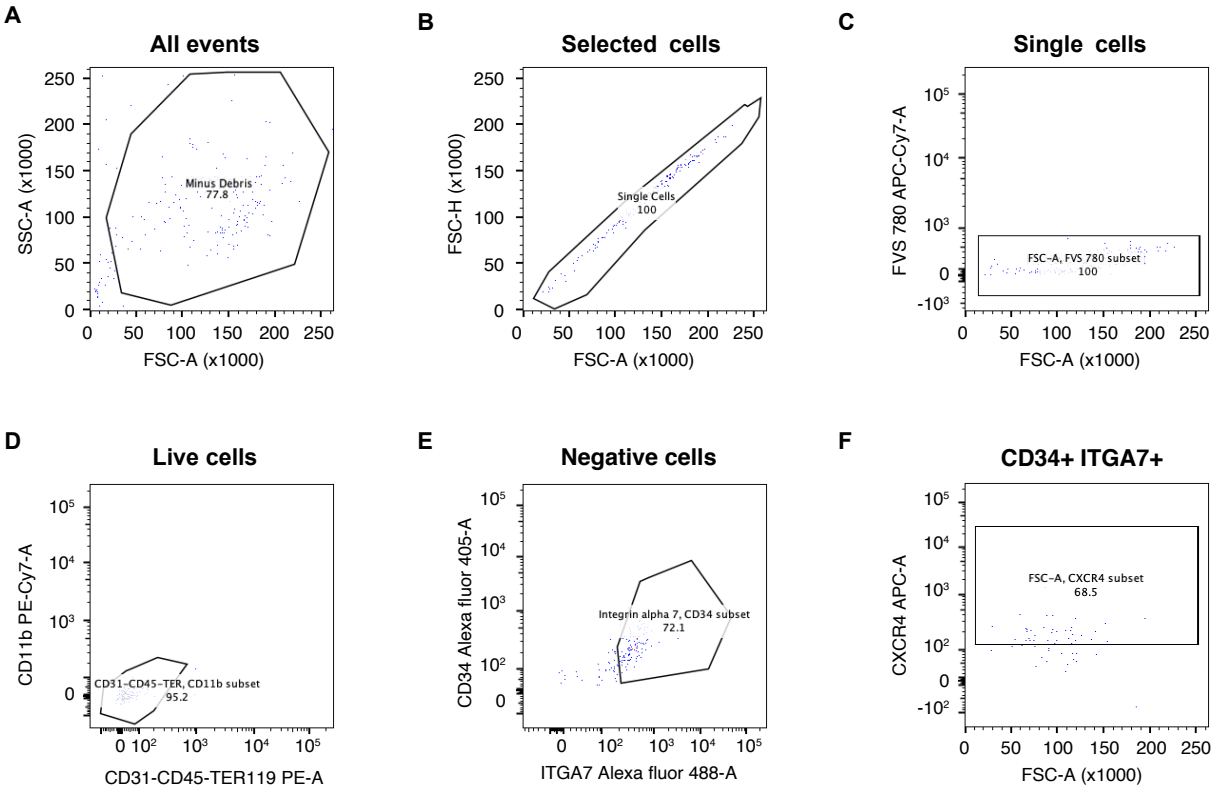

Supplementary Figure 1. Flow cytometry analysis of the cell preparation post-sorting.
A. Selection of the population of interest based on FSC-A and SSC-A parameters.
B. Single cells identification based on FSC-A and FSC-H.
C. Identification of living cells with fixable viability stain (FVS 780).
D. Negative cell selection based on CD11b, CD31, CD45 and TER119 antigens.
E-F. Positive cell selection based on CD34 and ITGA7 (E), as well as CXCR4 (F) antigens.
Gates are represented as black boxes.

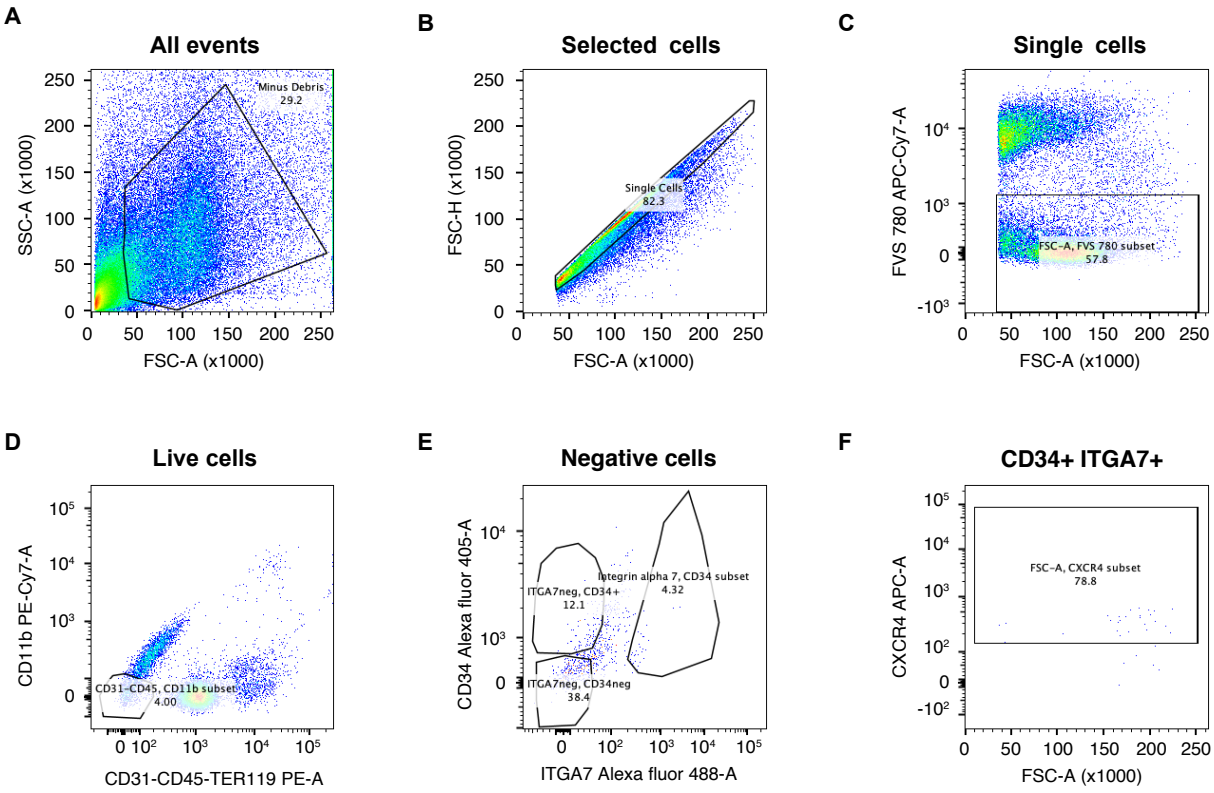

Supplementary Figure 2. Flow cytometer gating strategy for satellite cell sorting after digestion with 300 µL of Liberase TL.

A. Selection of the population of interest based on FSC-A and SSC-A parameters.

B. Single cells identification based on FSC-A and FSC-H.

C. Identification of living cells with FVS 780.

D. Negative cell selection based on CD11b, CD31, CD45 and TER119 antigens.

E-F. Positive cell selection based on CD34 and ITGA7 (E), as well as CXCR4 (F) antigens.

Gates are represented as black boxes.

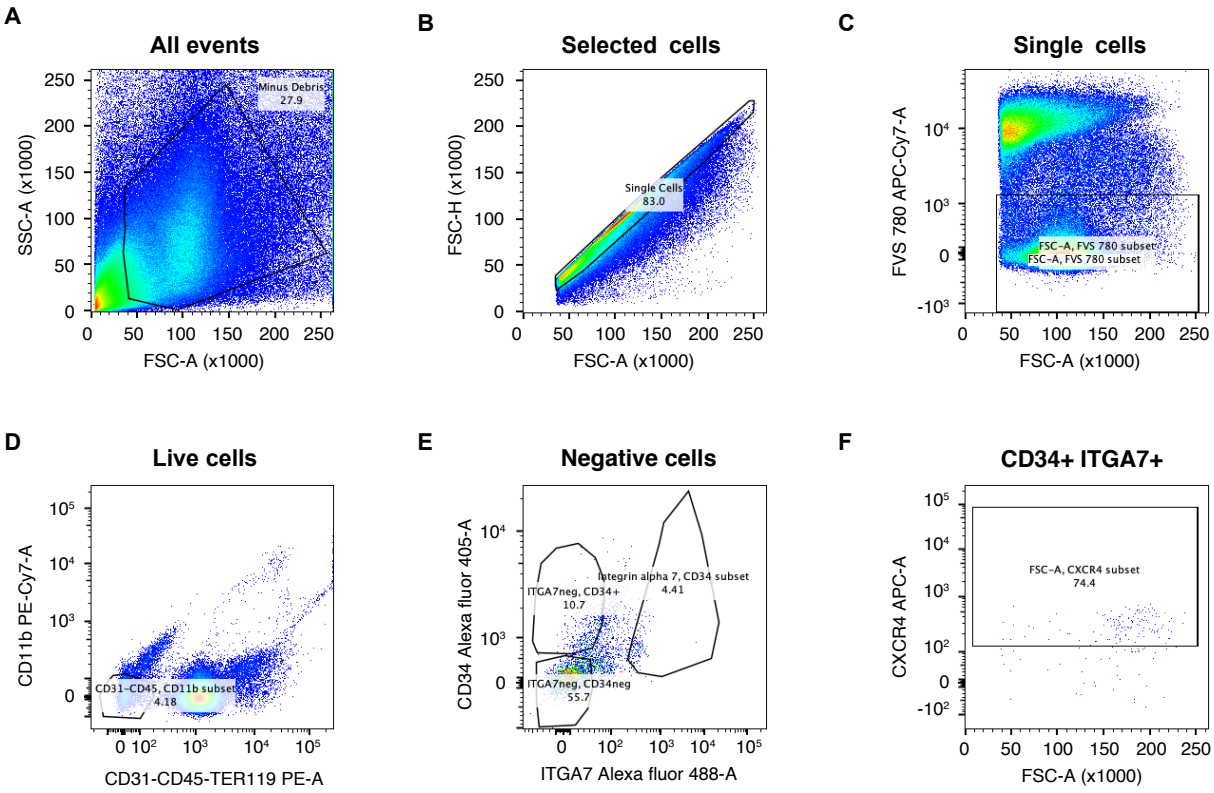

Supplementary Figure 3. Flow cytometer gating strategy for satellite cell sorting after digestion with 600 µL of Liberase TL.

A. Selection of the population of interest based on FSC-A and SSC-A parameters.

B. Single cells identification based on FSC-A and FSC-H.

C. Identification of living cells with FVS 780.

D. Negative cell selection based on CD11b, CD31, CD45 and TER119 antigens.

E-F. Positive cell selection based on CD34 and ITGA7 (E), as well as CXCR4 (F) antigens.

Gates are represented as black boxes.

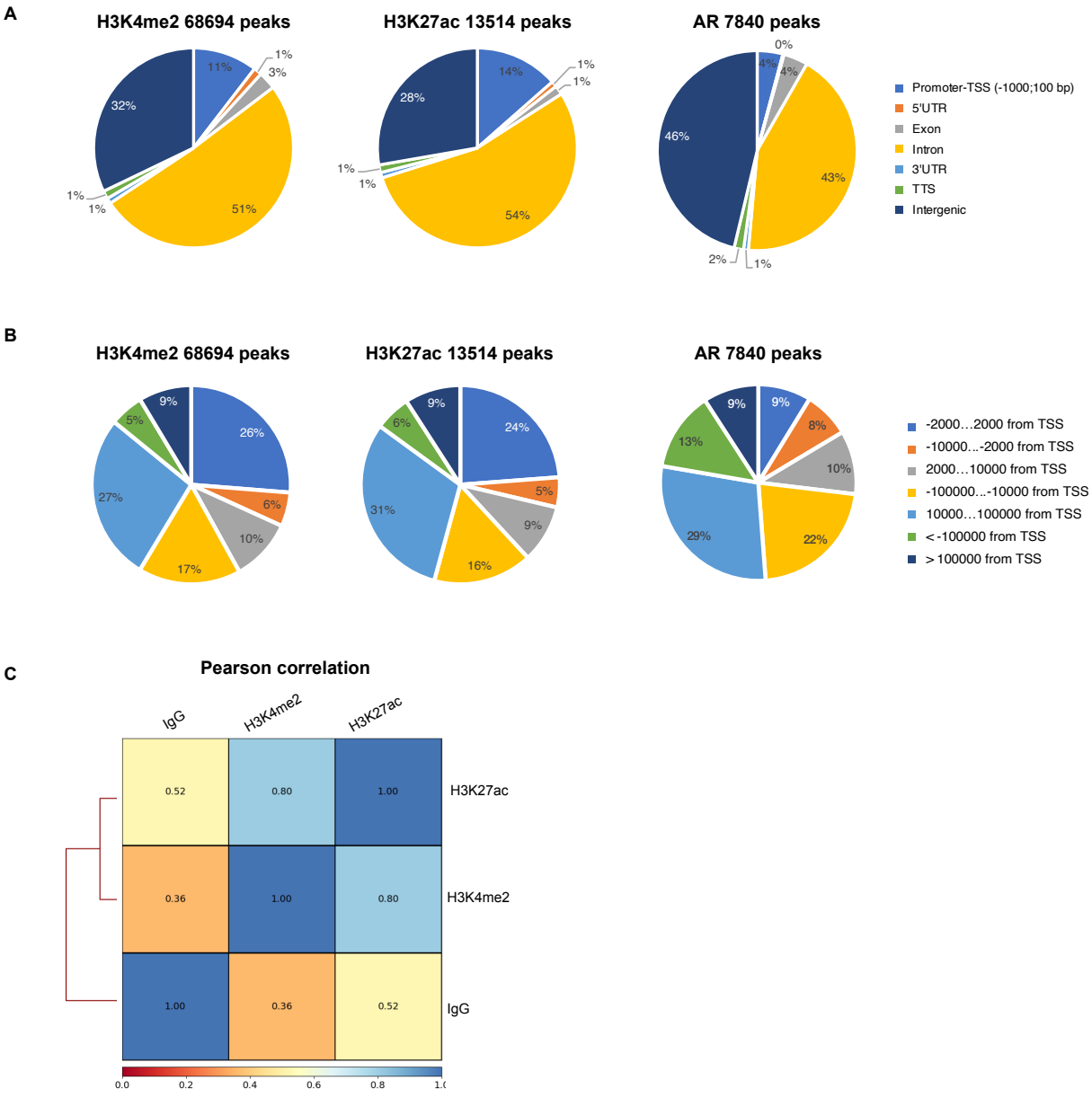

Supplementary Figure 4. Characterization of H3K4me2, H3K27ac and AR genomic locations.
A. Pie charts depicting the peak distribution of H3K4me2, H3K27ac and AR according to genome features in satellite cells.
B. Pie charts depicting the peak distribution of H3K4me2, H3K27ac and AR according to their distance to the nearest TSS in satellite cells.
C. Heatmap showing the Pearson correlation between H3K4me2, H3K27ac and IgG control.

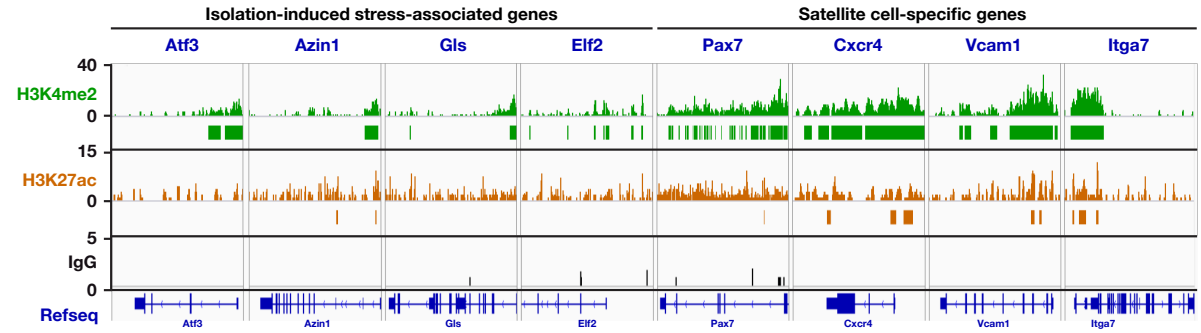

Supplementary Figure 5. Genomic profiles of satellite cell chromatin at stress-response induced genes. Localization of H3K4me2 and H3K27ac at indicated genes on chromatin of satellite cells. Immunoprecipitation with IgG was used as a negative control.

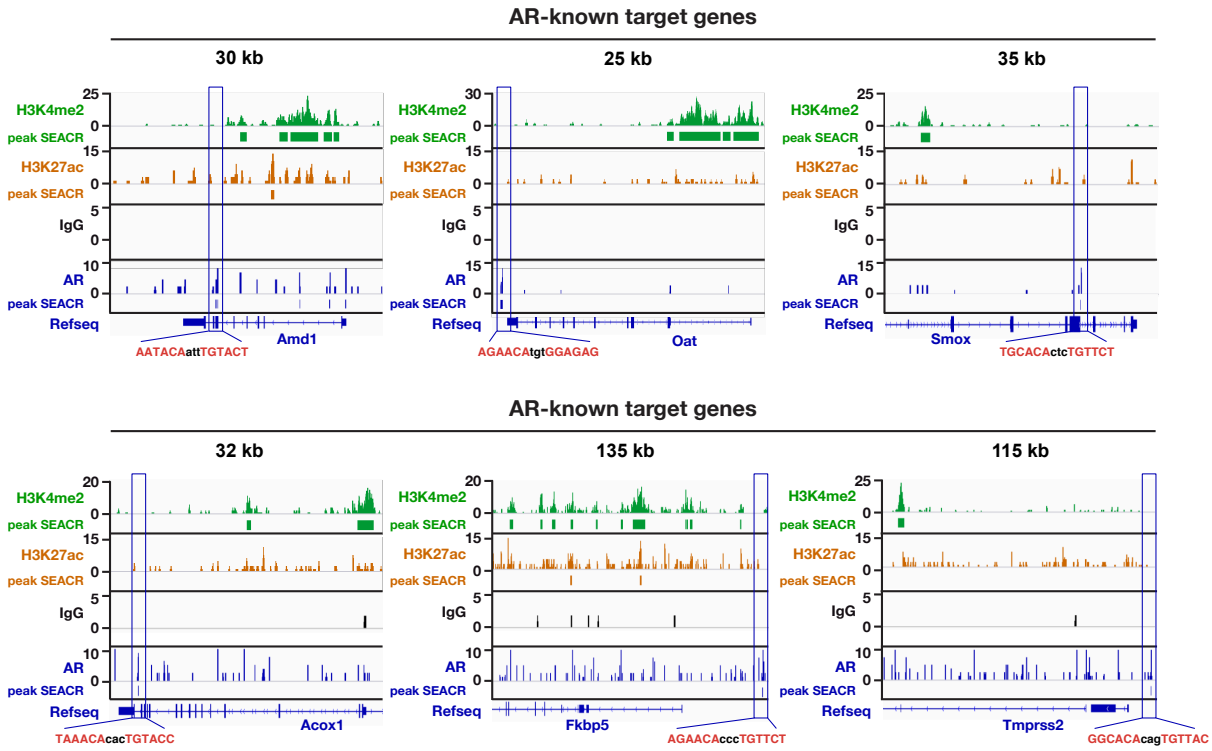

Supplementary Figure 6. Genomic profiles of satellite cell chromatin at known AR target genes. Localization of H3K4me2, H3K27ac and AR at indicated genes on chromatin of satellite cells determined by CUT&RUN. AR peaks are boxed in blue, and corresponding androgen receptor-responsive elements are presented below. CUT&RUN performed with IgG was used as a negative control.

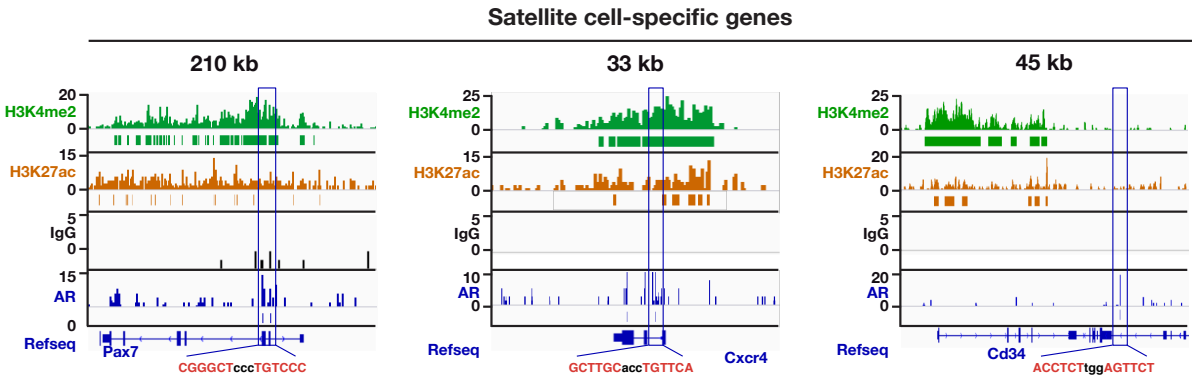

Supplementary Figure 7. Genomic profiles of satellite cell chromatin at their selectively expressed genes. Localization of H3K4me2, H3K27ac and AR at indicated genes on chromatin of satellite cells determined by CUT&RUN. AR peaks are boxed in blue, and corresponding androgen receptor-responsive elements are presented below. CUT&RUN performed with IgG was used as a negative control.